Research and Development Technical Report

ECOM - 4533

UTILIZATION OF ALUMINUM ALLOY ANODES FOR AN ELECTRO-CHEMICAL HEATER

AD A046116

S. Gilman
P. Bramhall
Electronics Technology & Devices Laboratory

September 1977

AD
DDC FILE COPY

DDC

RECEIVED
NOV 8 1977

B

ECOM

US ARMY ELECTRONICS COMMAND FORT MONMOUTH, NEW JERSEY 07703

NOTICES

Disclaimers

Disposition

SECURITY CLASSIFICATION OF THIS PAGE (When Data Entered)

REPORT DOCUMENTATION PAGE	READ INSTRUCTIONS BEFORE COMPLETING FORM

1. REPORT NUMBER	2. GOVT ACCESSION NO.	3. RECIPIENT'S CATALOG NUMBER
ECOM- 4533		Research and development

4. TITLE (and Subtitle)	5. TYPE OF REPORT & PERIOD COVERED
UTILIZATION OF ALUMINUM ALLOY ANODES FOR AN ELECTROCHEMICAL HEATER	Technical Report.
	6. PERFORMING ORG. REPORT NUMBER

7. AUTHOR(s)	8. CONTRACT OR GRANT NUMBER(s)
S. Gilman P. Bramhall	CA

9. PERFORMING ORGANIZATION NAME AND ADDRESS	10. PROGRAM ELEMENT, PROJECT, TASK AREA & WORK UNIT NUMBERS
US Army Electronics Command ATTN: DRSEL-TL-PR Fort Monmouth, New Jersey 07703	1L7 62724 AH 99 CA-003

11. CONTROLLING OFFICE NAME AND ADDRESS	12. REPORT DATE
US Army Electronics Command ATTN: DRSEL-TL-PR Fort Monmouth, New Jersey 07703	September 1977
	13. NUMBER OF PAGES
	29

14. MONITORING AGENCY NAME & ADDRESS(if different from Controlling Office)	15. SECURITY CLASS. (of this report)
34 p.	Unclassified
	15a. DECLASSIFICATION/DOWNGRADING SCHEDULE

16. DISTRIBUTION STATEMENT (of this Report)

Approved for public release;
distribution unlimited.

17. DISTRIBUTION STATEMENT (of the abstract entered in Block 20, if different from Report)

18. SUPPLEMENTARY NOTES

19. KEY WORDS (Continue on reverse side if necessary and identify by block number)

Electrochemical Heater   Magnesium Cell
Aluminum Cell   Aluminum Alloy Anodes
Magnesium-Saltwater Cell   Aluminum-Saltwater Cell

20. ABSTRACT (Continue on reverse side if necessary and identify by block number)
A magnesium/manganese dioxide cell has been developed for direct heating of field rations under short-circuit conditions. Although fast and convenient, the cell has the disadvantage of producing considerable hydrogen gas during its operation, thereby presenting a potential explosion hazard.

This report deals with an electrochemical analysis of the hydrogen evolution problem in the magnesium/manganese dioxide heater cell and with the exploration of aluminum alloys as low-gassing substitutes for magnesium in such a cell. The results reveal that, in the early period of discharge of a

(Cont on Reverse Side)

DD FORM 1473 EDITION OF 1 NOV 65 IS OBSOLETE
1 JAN 73

037620

Item 20 - Abstract - Continued

magnesium cell, most of the hydrogen is produced at the anode. Gas production becomes more significant at the cathode during the later period of cell discharge. The use of an aluminum alloy anode of a particular composition greatly reduces the problem of gassing at the anode and completely eliminates gassing at the cathode.

CONTENTS

FIGURES

CONTENTS

FIGURES (CONT)

TABLES

UTILIZATION OF ALUMINUM ALLOY ANODES
FOR AN ELECTROCHEMICAL HEATER

INTRODUCTION

If an electrochemical cell is short-circuited, its chemical energy is almost completely converted into heat via the various ohmic and non-ohmic polarizations occurring in the electrolyte and at both electrodes. The heat from such an "electrochemical heater" may be largely transferred, by thermal conduction, to any material with which it is in intimate contact. One advantage of such an electrochemical heat source over a purely chemical (e.g., thermite) one is that the reaction tends to proceed in a more gradual and controlled manner.

Electrochemical heaters utilizing aluminum and magnesium anodes and various cathodes have been developed for various applications.[1-4] In particular, Power Applications, Inc. (Valley Stream, L.I., NY), under sponsorship by the US Army Natick Laboratories, has developed an electrochemical heater for heating field rations which are sealed in plastic-aluminum laminated pouches.[5] The cell utilizes a Mg anode, a MnO_2 cathode, and a NaCl electrolyte. It accomplishes the desired heat transfer in a convenient time period (within 15 minutes) and requires no protective packaging during use because of the non-toxicity of its components. The cell has the disadvantage, however, of evolving a considerable volume of hydrogen gas as a by-product, the latter constituting a potential explosion hazard. It was the purpose of the present work to investigate whether the hydrogen production problem could be eliminated or minimized while preserving the good thermal characteristics of the present heater.

Two main approaches were made to the general problem. In the first, mechanical modifications of the Mg anode were investigated, in an attempt to minimize the amount of Mg incorporated into the anode. This is possible, for the present heater design, because a large percentage of the magnesium anode does not contribute to the useful heating process. Instead, that amount of magnesium undergoes slow corrosion, liberating hydrogen. The second approach involved identification of an aluminum alloy to replace the present Mg anode. This approach additionally required improvement of the present MnO_2 cathode.

EXPERIMENTAL PREPARATIONS/PROCEDURES

Preparation of Electrodes and Electrolytes

Anodes. The magnesium used in the flat cells, with the electrolyte pads, was "primary grade" (Dow) of 0.028 cm thickness in sheet form. Where

[1] W. C. Spindler, US Patent #3,207,149, Sep 21, 1965.
[2] F. P. Kober, US Patent #3,774,589, Nov 27, 1973.
[3] J. F. McCartney, US Patent #3,884,216, May 20, 1975.
[4] Technical Report #74-44-GP by Power Applications, Inc. on Contract No. DAAG-17-73-C-0250 with General Equipment and Packaging Laboratory, US Army Natick Laboratories, 31 Dec 1973.
[5] Technical Report #74-44-GP, op. cit.

measurements of current were not made, the Mg anode was stapled to the cathode through the electrolyte pad by the use of steel staples. Where sheets of reduced thickness were used, or external electrical connections were required, a mechanical contact was made to the outer surface of the magnesium sheet, using a nickel expanded metal screen (5 Ni 7-2/0 from the Exmet Corp.). The screen was cemented to the Mg with epoxy cement in a hydraulic press with heated platens (200 kilograms/cm^2 pressure at 135°C). A tab of screen was left on the sample and a heavy gauge tinned copper wire was soldered to it in such a way that no contact was possible between the solder connection and the electrolyte. For half-cell experiments with magnesium anodes in an excess of electrolyte, a 0.3 cm diameter rod of "sublime grade" (Dow) magnesium was used. The aluminum used in half-cell studies with excess electrolyte was 0.1 cm diameter wire of 99.99+% purity (Alfa Inorganics). The aluminum alloys used in both flat-cell (electrolyte pad) and in half-cell (excess electrolyte) studies were prepared by the Reynolds Metals Co. using procedures and heat treatments similar to those previously reported.[6] The alloys were prepared with high purity (99.992%) aluminum as a base; the aluminum was induction-melted, in air, in silicon carbide crucibles. All additions of pure metals were added at a temperature over 705°C and stirred to ensure homogeneity. The melts were degassed with gaseous chlorine and then semicontinuously cast into ingots using an aluminum direct chill caster. The ingots were cleansed by scalping the surfaces. They were then heat-treated for homogenization and cold-rolled to a thickness of 0.04 cm. Samples for use in flat cells (with electrolyte pads) were prepared with expanded nickel screens in the manner already described above. Samples of the 0.04 cm thick aluminum alloy sheets were prepared for use in half-cell experiments (with excess electrolyte) by pressure-cementing a nickel contact to the top of a 0.5 cm x 2 cm sample of the alloy sheets and by masking off the nickel with silicone rubber.

MnO$_2$ Cathodes. Electrodes were made, or obtained, with various formulations containing MnO$_2$, graphite, carbon black, graphite fibers, and current-collecting screens. Methods of preparation are reported below for four particular formulations:

(1) Electrodes of this formulation were developed[7] and supplied by Power Applications, Inc., Valley Stream, Long Island, NY. They were prepared by binding a mixture of MnO$_2$ (natural ore containing 74% MnO$_2$ obtained from the A Man Co., Inc., Philadelphia, PA), carbon black (cabot XR-72), and Fullers earth (in the weight ratio of 10:2:1), with polytetrafluoroethylene emulsion, to a 20 x 20 mesh steel grid. The completed cathode was of 0.05 cm thickness and contained 0.035 g of MnO$_2$ ore per square centimeter of electrode area.

(2) This formulation was based on formulations reported by K. Kordesch.[8] A mixture of MnO$_2$ ("chemical MnO$_2$ ore" from Manganese Chemical Corp.), graphite powder (Fisher Scientific Co.). and carbon black (Shawinigan B/A-147) in proportions 43:5:1 were ball-milled for two hours using glass balls. The mixture was then blended with Fullers earth and graphite fibers

[6] D. S. Keir, M. J. Pryor, and P. R. Sperry, J. Electrochem. Soc. <u>114</u>, 777 (1967).
[7] Technical Report #74-44-GP, op. cit., p. 1.
[8] K. Kordesch, US Patent #3,945,847 March 1976.

in proportions 100:5:1. The blend was then mixed with a 5% solution of lucite in trichloroethylene (percentage of lucite in final dry mixture was 2.5%), applied to an etched 20 x 20 gauge stainless steel screen and air-dried. The completed electrode contained 0.07 g of MnO_2 ore per square centimeter of electrode area.

(3) Electrodes of this formulation were developed[9] and supplied by K. Kordesch (Union Carbide Corp.). They were of similar formulation to the ones described in (2) above but utilized Tekkosha brand MnO_2, three times the graphite fiber content, and no Fullers earth. The finished electrodes were 0.1 cm thick and contained 0.17 g of MnO_2 per square centimeter of electrode area.

(4) This formulation was prepared using the ball-milled mixture of MnO_2, graphite, and carbon black mentioned in formulation (2) above. The mixture was dry-pressed into a porous nickel matrix (45 pore, 0.41 cm thick "Foametal" from Hogen Industries, Willoughby, Ohio) in a manner similar to that reported previously.[10] The final structure was 0.1 cm thick and contained 0.2 g of MnO_2 per square centimeter of electrode area.

Except in stapled cells, electrical contact was made to the cathodes by welding a lead to a tab of exposed screen and insulating in such a way that contact between the lead and the electrolyte was avoided.

Electrolytes. For experiments with complete flat cells ("electrochemical heater" experiments), the cell was assembled in the dry state, using 0.165 cm thick "Webril R-2801" (Kendall Mills) impregnated with NaCl ($0.037 g/cm^2$). Such cells were "activated" just before use by adding an excess of water for 10 seconds and then draining off. The same electrolyte arrangement was used in the voltage-sweep experiments on cathodes. Experiments on fully-immersed anodes and cathodes were performed using a solution of NaCl made by saturating distilled water with reagent grade salt at room temperature.

Procedures for Making Electrochemical and Hydrogen-Release Measurements

Stapled Electrochemical Heaters ("Hot Sheets"). The complete "hot sheets" (Mg/MnO_2 electrochemical heaters) developed by Power Applications, Inc. comprise two cell sections, each 7 cm x 10.5 cm in size, connected with a section of steel screen for convenience in wrapping around a standard five ounce plastic-encased military field ration. Each cell section is made by stapling together an anode of primary magnesium, a salt-impregnated separator pad, and a cathode (formulation (1) above). Such cells are activated by steeping in water for 10-15 seconds and draining off excess water. Hydrogen release experiments were performed on such cells (with and without a food sample) by quickly placing in a small vacuum dessicator and collecting hydrogen over water in a graduated cylinder. Modified "hot sheets," using Mg anodes of reduced thickness were made from parts of the as-received cells. The Mg anodes were chemically etched, bonded to expanded nickel screen, as described above, and re-assembled by stapling.

---

[9] K. Kordesch, US Patent #3,945,847, op. cit., p. 2.
[10] H. F. Hunger and J. E. Ellison, J. Electrochem. Soc. 122, 1288 (1975).

<u>Unstapled Electrochemical Heaters</u>. An external current lead, rather than staples, must be used for studies on "hot sheets" where measurements of current and electrode potential are required. Cells with 5.08 cm x 5.72 cm cathodes and anodes were assembled for studies on the standard "hot sheet" ($Mg-MnO_2$ cell) and with 1 cm x 1 cm electrodes (to conserve materials) for the study of cells utilizing experimental anodes and cathodes. The cells were assembled in a gas-tight lucite fixture of very small internal volume in which rubber pads maintained pressure on the cell components and acted as a heat sink. The temperature at the anode-rubber interface was monitored with a chromel-alumel thermocouple when desired. All the electrodes used in these experiments were fabricated with screens to which heavy current leads were soldered inside the lucite fixture and those leads were also useful in supporting and positioning the electrodes in the cell. The cells were fabricated using the salt-filled Webril electrolyte pad described above. The pad was left oversize at one end and 0.3 cm wide strips of MnO_2 cathode (formulation (1)) were placed in the same planes as the anode and cathode with a 0.1 cm gap between each strip and the adjacent electrode. These served as "dry" reference electrodes for the adjacent anode or cathode. The recorded potentials were then converted to "potentials vs the saturated calomel electrode," by subtracting 0.41 volt, which takes into account the typical open-circuit voltage of cathode formulation (1). The external connection between the anode and cathode was made by means of a calibrated 0.01 Ω shunt through which the "virtual" short circuit current was monitored continuously by means of a strip chart recorder (Hewlett Packard #7100B). Simultaneous recordings were made of the anode and cathode potentials relative to their respective reference electrodes. The volume of hydrogen gas evolved from a cell was determined using a gas buret. As for the standard "hot sheet," water was added to the electrolyte pad by flooding a cell with excess water for 15 seconds and draining off the excess.

<u>Measurement of Anode Polarization and Hydrogen Gas Evolution at Fully-Immersed Anodes</u>. Anode polarization was studied using wire or 0.5 cm x 2 cm foil samples, prepared as specified above. The experiments were performed in a glass-stoppered, thermostatted, (25°C) three-compartment cell with a reference saturated calomel electrode (SCE) and a platinized platinum counter electrode. The electrolyte was a saturated solution of sodium chloride; 200 cm^3 of the electrolyte were required for the working electrode compartment and that volume was renewed after each determination. The polarization (current-potential) curves were recorded on an X-Y recorder (Hewlett Packard #7047A) while applying a positive-going potential scan (speed of 0.001 volts/second) using a potentiostat (Tacussel #PIT20-2A) and signal generator (Tacussel #GSTP-2). The sweeps were reversed manually after reaching a top current of 200 mA/cm^2.

Gas evolution was measured for similar anodes under constant-current conditions. A small funnel-shaped glass mantle was positioned directly over the electrode and served to collect the gas as formed. The gas then flowed into a bubble flowmeter of either 1 or 10 cm^3 volume (chosen according to anticipated rate of gas evolution) and the level of the bubble recorded at one minute intervals. With the 1 cm^3 flowmeter, flow rates as small as 2.2×10^{-4} cm^3/second (equivalent to an electrochemical H_2 evolution rate of 2 mA) can be read with 90% accuracy within three minutes after initiating the flow, and rates down to 1.1×10^{-4} cm^3/sec

(1 mA) can be read accurately after five minutes. The accuracy was tested by generating H_2 at a platinum electrode (with 100% efficiency). The three and five minute delay intervals cited above probably correspond to the very slight lowering of the electrolyte meniscus (and buildup of gas pressure) required to overcome inertia of the soap film in the bubble flowmeter.

Measurement of Polarization and Hydrogen Evolution of Fully Immersed Cathodes. The procedures used for studying MnO_2 cathodes in an excess of saturated NaCl solution were identical to those described directly above for anodes, except for the type of signal impressed on the cathode. In this case, a pre-selected constant potential was applied to the electrode ("potential-step" method) and the resulting current-time trace was recorded on a strip chart recorder (Hewlett-Packard #7100B). A fresh sample of electrode was required for each new potential imposed. Hydrogen gas is evolved at a MnO_2 electrode at sufficiently negative potentials. The rate of gassing was measured under "potential-step" conditions for cathode formulation (1).

Measurement of Polarization at Cathodes Using an Electrolyte Pad. For purposes of fast "screening" of new electrolyte formulations, polarization curves were measured using a cathodic-going potential sweep. Since many of the electrode formulations were found to give better results when mechanically compressed (thus improving contact between the MnO_2 and the current collector), such experiments were performed using the salt-impregnated Webril pad described above, and a Mg "counter-electrode" in an arrangement similar to that described above for "unstapled electrochemical heaters."

RESULTS AND DISCUSSION

Thermodynamic Considerations

Table 1 presents the reaction equations and corresponding thermodynamic quantities for the chemical processes anticipated in Mg and Al cells utilizing MnO_2 cathodes.[11,12] The standard enthalpy, ΔH^o, the standard free energy, ΔF^o, those latter quantities divided by the number of equivalents ($\Delta H^o/n$ and $\Delta F^o/n$), and the standard cell potential E^o were calculated using standard enthalpies and free energies of formation.[13] Reaction equations for Cells (1) and (3) of Table 1 correspond to coulombically efficient utilization of both plates of each cell. The equations for Cells (2) and (4) are for the reactions producing hydrogen. The hydrogen may be produced at either the anode (corrosion) or the cathode (cathode gassing). The most relevant quantities for heat-production purposes are the enthalpies, rather than the free energies. Furthermore, reference to the values of $\Delta H^o/n$ is useful if we wish to compare the reactions for the same "internal current" of the cell. Since the values of ΔF^o and ΔH^o are almost identical, the values of E^o are almost as valid for purposes of comparison as

[11] D. S. Keir, M. J. Pryor, and P. R. Sperry, op. cit., p. 2.
[12] The Primary Battery, Volume 1, edited by G. W. Heise and N. C. Cahoon (John Wiley & Sons, Inc., NY, 1971).
[13] Handbook of Chemistry and Physics, 53rd Edition, Chemical Rubber Co., Ohio, 1972.

Table 1. Thermodynamic Quantities of Cell Reactions

Cell	Reaction	ΔH^o (kcal)	ΔF^o (kcal)	$\Delta H^o/n$ (kcal/eq.)	$\Delta F^o/n$ (kcal/eq.)	E^o volts
(1) Mg/MnO_2	$Mg + 2\ MnO_2 + H_2O \longrightarrow Mg(OH)_2 + Mn_2O_3$ (β-form) (α-form) (α-form)	-135.8	-133.5	-67.9	-66.8	2.88
(2) Mg/H_2	$Mg + 2\ H_2O \longrightarrow Mg(OH)_2 + H_2$	-84.4	-85.9	-42.2	-43.0	1.86
(3) Al/MnO_2	$2\ Al + 6\ MnO_2 + H_2O \longrightarrow Al_2O_3 \cdot H_2O + 3\ Mn_2O_3$ (β-form) (Hydrated γ-form) (α-form)	-351.9	-351.0	-58.7	-58.5	2.54
(4) Al/H_2	$2\ Al + 4\ H_2O \longrightarrow Al_2O_3 \cdot H_2O + 3\ H_2$ (Hydrated γ-form)	-197.7	-208.2	-33.0	-34.7	1.50

those of $\Delta H^o/n$. From the values of E^o we may, therefore, conclude that, for identical cell "internal current" and with no hydrogen evolution, the Al/MnO_2 cell is 12% less energetic than the Mg/MnO_2 cell. On the other hand, much of the total "internal current" of the present Mg cell is directed into the far less efficient hydrogen evolution reaction (Reaction Number 2, Table 1). If this reaction were eliminated, it could more than compensate for the 12% loss.

Evaluation of the Mg/MnO_2 "Hot Sheet"

Hydrogen Evolution and Mg Utilization Under Practical Conditions. A standard "hot sheet" was activated and placed in a cardboard insulator container, and the entire assemblage was quickly placed in the apparatus for measurement of released hydrogen gas volume. The same experiment was also repeated without a food package. The hydrogen-release results are plotted on Figure 1. The difference in the results with and without the food package is attributable to the difference in cell internal temperature for the two conditions. Without heat transfer to the package, the cell runs warmer, the internal impedance is lower, and the internal short-circuit current is greater. Using the hydrogen evolution data as an indication of overall rate of heat evolution, it can be judged that most of the heat transferred to the food package is produced during the first few minutes. In practical use, the cell is normally kept in contact with the food for approximately 15 minutes, during which period approximately 800 cc of H_2 are produced, with 1-1/2 additional liters of gas being released in the next 16 hours. The latter can be largely eliminated by purely mechanical modification of the Mg electrode. In another experiment, a "hot sheet" was dismantled, the two Mg electrodes were weighed, and the cell reassembled and discharged with a food packet. After again disassembling the cell and washing, the Mg weight loss was found to be 2.95 g or 41% of the original weight. This shows that 59% of the Mg does not contribute to useful heating, but is responsible for the long-term hydrogen release problem. If all of the 2.95 g of Mg consumed in the first 15 minutes reacted via reaction equation (2) of Table 1, then 2,717 cc of H_2 would be produced. Since 790 cc are actually generated, the cell is 29% inefficient (i.e., 29% of reaction proceeds via equation (2)) in the first 15 minutes. Furthermore, based on the amounts of hydrogen released and Mg consumed, we may calculate the heat released in the first 15 minutes from the values of ΔH^o in Table 1; that value is 11.6 kcal. By comparison, the maximum heat actually transferred to a food packet in the same time may be estimated as 9.6 kcal, the remainder being dissipated into the air.

Electrochemical and Gas Evolution Measurements on Unstapled Electrochemical Heaters. A Mg/MnO_2 cell was assembled in a lucite fixture, utilizing standard "hot sheet" parts. The electrodes were 5.08 cm x 5.72 cm in size. Pressure was maintained on the cell by the rubber pads in the fixture. Figure 2 presents the temperature at the Mg/rubber interface, the electrode potentials (referred to a saturated calomel electrode (SCE)) and the "virtual" short-circuit (across a 0.01 Ω load) current density, I_{SC}, as measured after "activating" the cell with water for 10 seconds. The
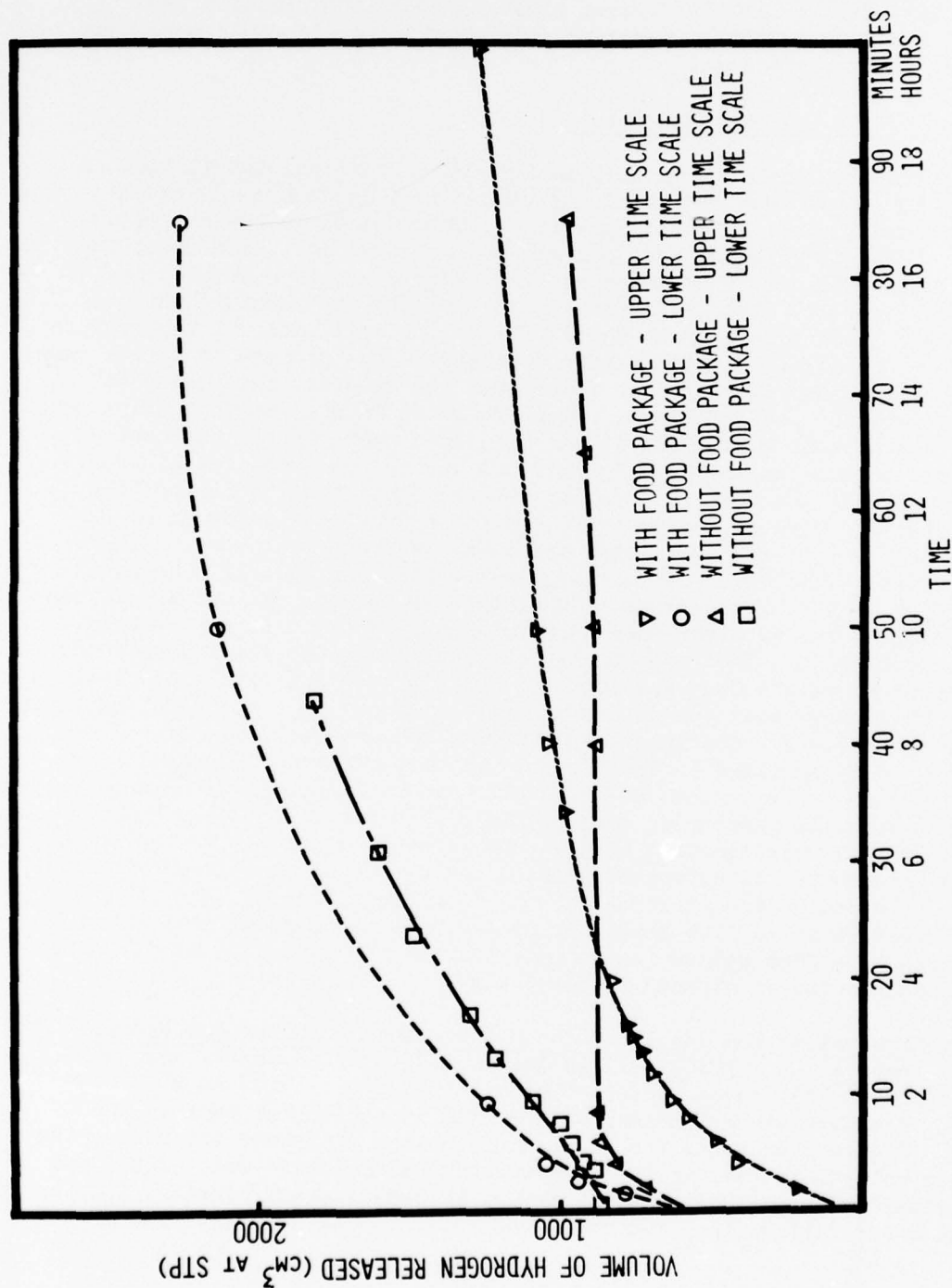
7

Figure 1. Results of Hydrogen Gas Release Experiments
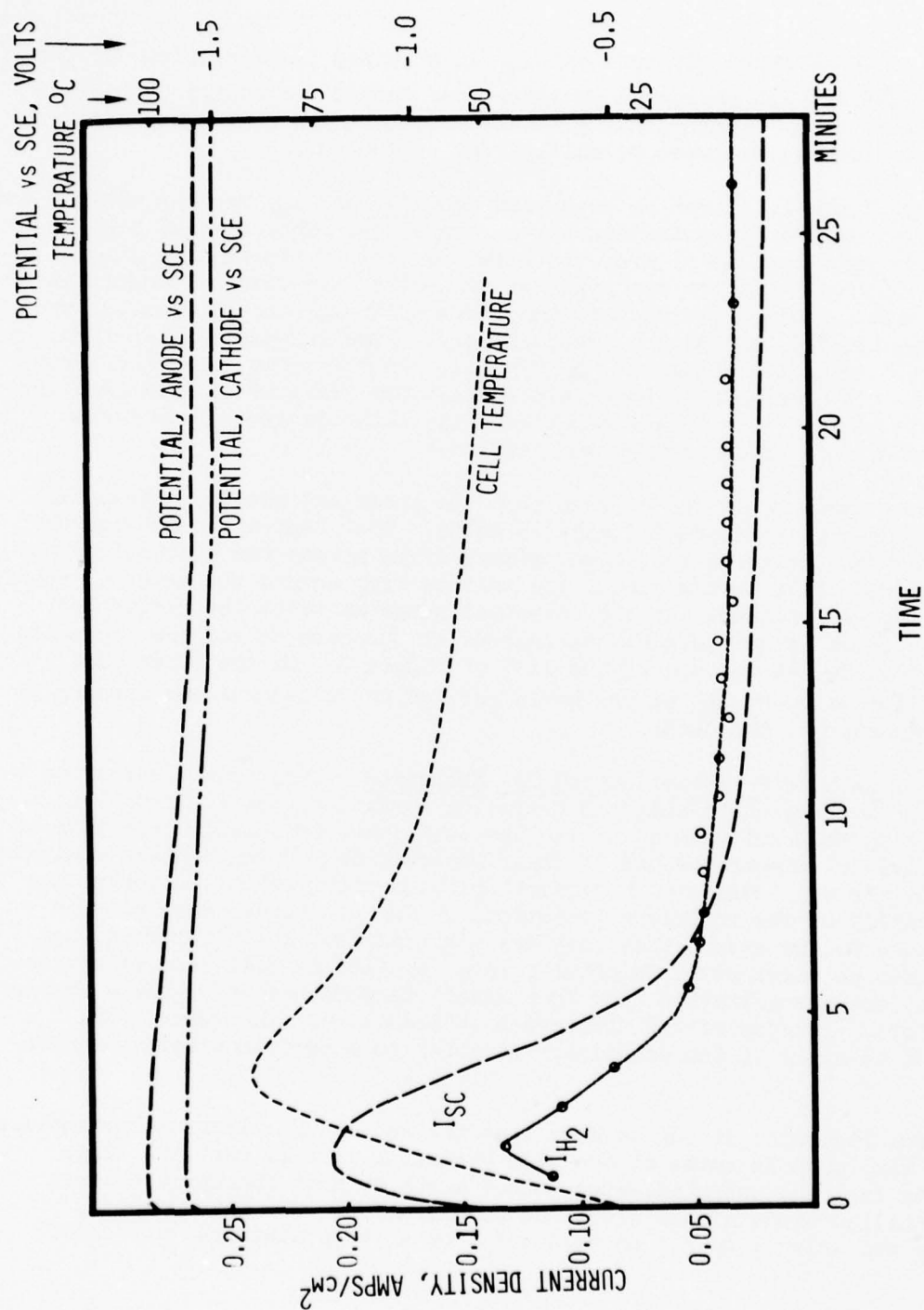from a Standard Mg/MnO2 "Hot Sheet"

8

Figure 2. Operating Characteristics of an Instrumented Mg/MnO$_2$ Electrochemical Heater With Standard "Hot Sheet" Parts

6

measured volumes of hydrogen gas released were converted to an equivalent current density, I_{H_2}, by using the formula:

$$I_{H_2} = 2 \cdot \frac{\Delta V}{\Delta t} \cdot \frac{F}{22.4} \tag{1}$$

Where F is the Faraday constant and I_{H_2} is obtained in amperes/cm^2 if the gas flow, $\Delta V/\Delta t$, is expressed in liters per second per square centimeter of electrode area. Corresponding total currents for a full-sized standard "hot sheet" may be obtained by multiplying by 160 cm^2.

From Figure 2, it can be seen that both I_{SC} and I_{H_2} reach a maximum and decline within the first few minutes of operation. The initial high current is probably useful from the point of view of providing a strong initial driving force for the transfer of heat to the work. Integration of the I_{SC} and I_{H_2} plots yields the number of equivalents of Mg reacting via reactions 1 and 2, of Table 1, respectively. Heat release may, in turn, be calculated using the values of $\Delta H^O/n$ given in the table. For the first 15 minutes, the calculated heat release is 0.076 kcal/cm^2 or 12.2 kcal for a 160 cm^2 heater, in good agreement with the value derived above for a practical heater--food package combination.

From Figure 2, it can be seen that the anode and cathode potentials tend to converge to approximately 1.5 volts. The separation between the two potentials reflects resistive voltage drops across the electrolyte pad and the oxide film on the anode, the voltage drop across the external shunt having been eliminated. In the potential range at which the electrodes operate, there is considerable H_2-release at the cathode and that accounts for most of I_{H_2} at the end of the plot of Figure 2. On the other hand, most of the value of I_{H_2} at the early part of the discharge corresponds to gas production at the anode.

MnO_2 Cathode Polarization and Gas Evolution. The results appearing in Figure 2 correspond to only one operating condition (short circuit) of a complete Mg/MnO_2 cell and is of limited usefulness in detailed analysis of the individual electrodes and of their interaction. More detailed analysis requires the application of more sophisticated electrochemical techniques to the study of the individual electrodes. The electrodes must also be simplified to the extent that they are miniaturized, fully immersed (hot sheet uses an electrolyte "blotter") in a solution of well-defined concentration, and thermostatted (the "hot sheet" temperature undergoes a complex variation). Because of the difference in conditions, the results are expected to apply to the practical situation in a semiquantitative manner only.

From Figure 2, it can be seen that the individual electrode potentials do not vary much in spite of the wide variation in cell current. This suggests that the potential-step method might be most appropriate for a more detailed study of the electrode polarization. For this purpose, samples measuring 1 cm x 1 cm were cut from a large standard "hot sheet"

10

cathode and individually immersed in a saturated solution of NaCl. The area of each sample is taken as 1 cm^2 despite the fact that both sides are exposed, since the bulk of the porous cathode is utilized rather than its surface (the reverse is true for anodes). For each sample, a different fixed potential was applied and the current-time trace recorded. Points taken from the traces are plotted on Figure 3. From the figure it can be seen that, for time durations at constant potential of less than one minute, the current tends to increase with decreasing potential. For longer time durations, a plateau value occurs in the lower potential range. A second rise in current follows the plateau at decreasing potentials. The results can be interpreted as follows, based on the observation[14] that the cathodic reduction of MnO$_2$ tends to be diffusion-controlled soon after the beginning of the process:

(1) At short elapsed time, including up to 12 seconds, the reduction is only partially diffusion-limited and hence shows considerable potential-dependence over the whole potential range.

(2) After sufficient charge has passed, the reduction process becomes solid-state diffusion-controlled and, therefore, exhibits a current plateau. Referring to the one minute points, a plateau is evident from -1.0 V to -1.5 V. At less cathodic potentials than -1.0 V, the previous activation controlled current was not sufficiently high to result in diffusional control after one minute. At more cathodic potentials than -1.5 V, the current rise is due to electrolytic evolution of H$_2$.

(3) As the reduction time increases, diffusional control extends to less cathodic potentials, and the onset of H$_2$ evolution is more easily distinguished (potentials as positive as -1.3 V).

To confirm that hydrogen is evolved at the more cathodic potentials, a sample of electrode was polarized at -1.4 V for 10 minutes and gas evolution measured using a flowmeter, allowing six minutes at each potential. The gas evolution rates (measured at 100 second intervals) were found essentially time-independent, as might be expected for an electrocatalytic process. Average rates, converted to currents by means of Equation (1), are plotted on Figure 3. The results reveal that H$_2$ evolution is measurable at -1.3 V and that it accounts for virtually all of the cathodic current at more cathodic potentials after a few minutes of polarization. The reversible potentials (versus a saturated calomel electrode) of the two processes, which may occur at the MnO$_2$ cathode, appear in Table 2 (i.e., a and b). The expressions for the standard potentials were taken from reference 15. The pH of the NaCl electrolyte should be 7.0 initially, and should eventually reach 10.45 when thoroughly mixed and saturated with Mg(OH)$_2$.[15] In addition, transient high and low values of pH at cathode and anode, respectively, are likely during high current surges. Since the reversible potentials, from Table 2, for reaction (a) at pH 7 and pH 10.45 are quite positive, it is apparent that MnO$_2$ (Figure 3) is being reduced irreversibly

---

[14] F. Kornfeil, J. Electrochem. Soc. 109, 349 (1962).

[15] M. Pourbaix, Atlas of Electrochemical Equilibria in Aqueous Solutions, Pergamon Press, NY, 1966.
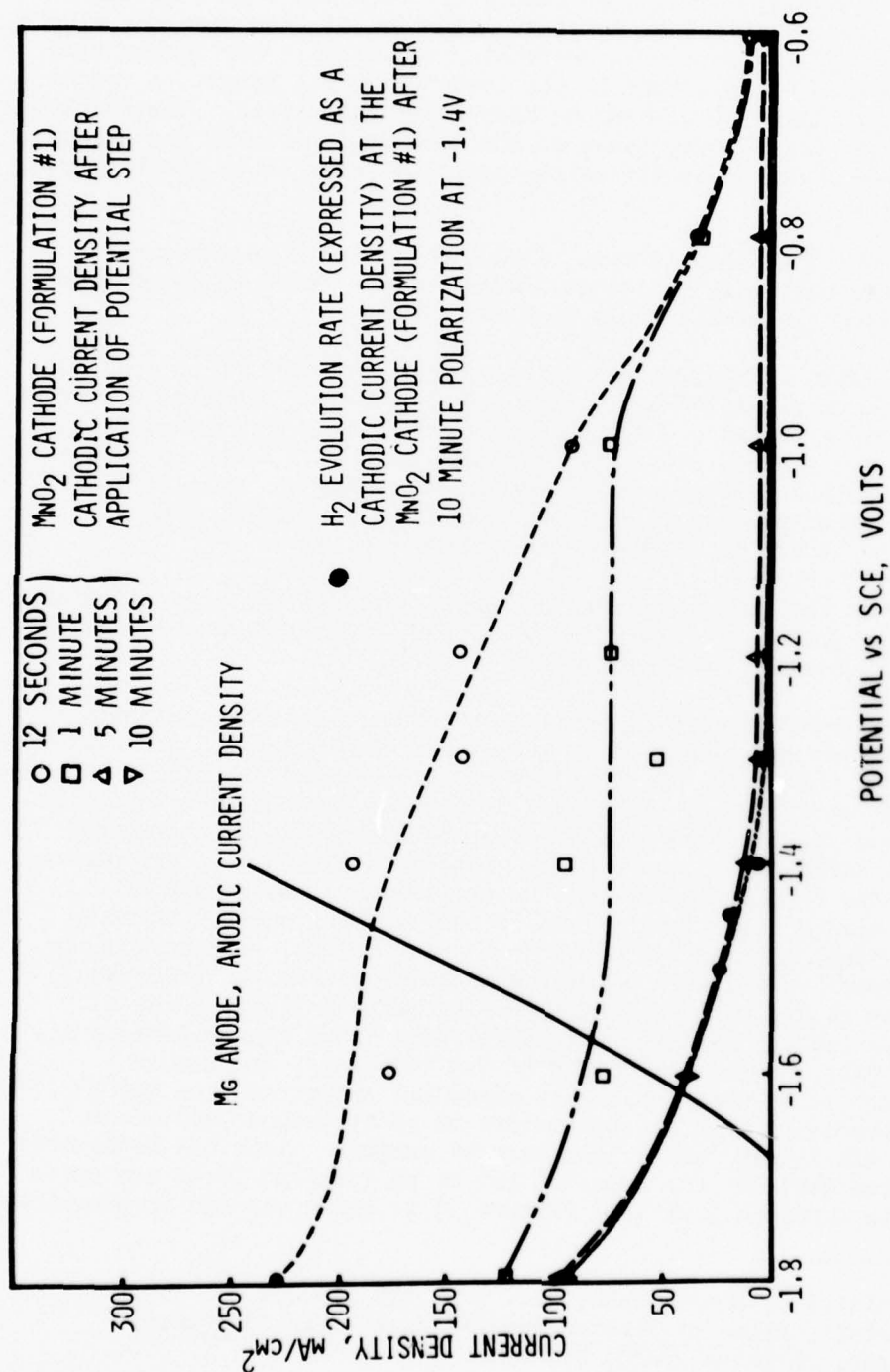
Figure 3. Polarization Behavior of Fully Immersed Mg Anodes and Standard MnO₂ Cathodes in Saturated NaCl Solution

12

Table 2. _Thermodynamic Reduction Potentials at 25°C_

Electrode Reaction	Standard Potential † Volts	Reversible Potential vs SCE (Volts)		
		pH 6.1*	pH 7.0	pH 10.45**
a) $2 MnO_2 + 2e^- + H_2O \rightleftharpoons Mn_2O_3 + 2(OH^-)$ (β-form) (α-form)	$1.014 - 0.0591\ pH$	0.417	0.364	0.160
b) $2H_2O + 2e^- \rightleftharpoons H_2 + 2(OH^-)$	$-0.0591\ pH$	-0.591	-0.650	-0.853
c) $Mg(OH)_2 + 2e^- \rightleftharpoons Mg + 2(OH^-)$	$-1.862 - 0.0591\ pH$	-2.102	-2.512	-2.715
d) $Al_2O_3 \cdot H_2O + 2H_2O + 6e^- \rightleftharpoons 2\ Al + 6(OH^-)$ (Hydrated γ-form)	$-1.505 - 0.0591\ pH$		-2.155	

†   Standard potentials are referenced to the normal hydrogen electrode.

*   pH of a saturated solution of γ-aluminum oxide is 6.1.

** pH of a saturated solution of $Mg(OH)_2$ is 10.45.

and that improved reduction kinetics would shift the curve to the right on the potential axis. For the H_2-evolution process (reaction (b), Table 2), it can be seen that gas evolution could begin at potentials as positive as -0.65 volts. The observation that no appreciable gassing occurs until -1.3 V largely reflects the fact that carbon (which is present for its electronic conduction properties) is a poor electrocatalyst for the hydrogen evolution reaction.

Mg Anode Polarization and H_2 Evolution. Unlike the situation for the MnO_2 electrode, the polarization of the fully-immersed Mg anode was found to change only slightly with time when held at constant potential. Hence, for Mg, and the various Al alloys to be discussed later, polarization was measured by applying a positive-going linear potential sweep (sweep speed = 0.001 volts/second) and measuring the current; the result is plotted in Figure 3. For a short-circuited cell, neglecting electrolyte resistance, the short-circuit current and electrode potential at any instant are determined by the point of intersection of the Mg anodic polarization curve with the appropriate MnO_2 cathodic polarization curve. The intersections of Figure 3 predict a drop in current from the 200 mA/cm^2 level in the first 12 seconds, to below the 50 mA/cm^2 level in 10 minutes, with that sharply declining current attributable entirely to cathode polarization. The long-term currents (according to Figure 3) are supported almost entirely by hydrogen evolution. Finally, Figure 3 predicts a moderate drift in the electrode potentials, to more cathodic potentials, conforming to the shape of the anodic polarization curve. This predicted behavior holds, in part, for the more complicated conditions of Figure 2. Those conditions are more complicated since they involve the use of an electrolyte pad, the in situ formation of a small volume of electrolyte, large variation of the internal temperature, and pH of the electrolyte. Nevertheless, Figure 2 does exhibit approximately the expected type of current decay after the current peak is passed. The initial rise in current probably corresponds mainly to the "voltage delay" phenomenon normally encountered[16] when a heavy load is first applied to the normally passive Mg anode. The drift of the electrode potentials is small, as expected, but is towards anodic, rather than cathodic potentials, probably signaling increased polarization of the Mg anode as the electrolyte is saturated with product under the conditions of minimal electrolyte volume. A very significant conclusion, based on Figure 3, is that shifting of the anodic curve to the right would tend to eliminate H_2 evolution at the cathode, the latter being the major source of H_2 evolution after the first ten minutes of cell operation. H_2 evolution at a pure Mg rod, fully immersed in saturated NaCl solution, is reported in Table 3. The quantities reported in Table 3 are the percentages of the total "internal" currents at the anodes which produce hydrogen, as obtained from Equation 2:

$$\text{Percentage } H_2 \text{ Evolution} = 100 \ I_{H_2}/(I + I_{H_2}) \qquad (2)$$

Where I_{H_2} is obtained from Equation (1), and I is the electrical current flow through the cell's external circuit. Percentages of hydrogen

---

[16]
J. L. Robinson and P. F. King, J. Electrochem. Soc. **108**, 36 (1961).

evolution similar to those reported for the pure Mg half cell can be calculated for the short circuited heater, for the few minutes of operation (Figure 2), if it is assumed that most of the H_2 evolved at that time is generated at the anode. This range of percentages (37%-45%) is higher than reported for $MgCl_2$ electrolytes[17] (approximately 30% at the higher current densities) probably reflecting the more corrosive nature of the present electrolyte.

Improvement of the Mg/MnO_2 Hot Sheet by Mechanical Means

In a previous section, it was shown that only approximately 40% of the metal content of the Mg anode is presently utilized for useful heating, the slow dissolution of the remainder being responsible for the long-term evolution of a relatively large volume of hydrogen. The long-term gas evolution can obviously be eliminated by efficient utilization of a smaller amount of the metal. In the present construction, 0.028 cm thick Mg is used, electrical contact being made with a number of steel staples. In our experimental "hot sheet," 0.017 cm thick Mg was made by chemically etching the thicker stock. By bonding the thin sheet to Ni exmet, both good lateral electronic conduction and physical integrity of the anode were maintained during discharge. A fully-sized "hot sheet" was constructed in the usual way using the standard cathode and electrolyte pad. The experimental heater was activated in the usual way and assembled with a food package. The hydrogen evolved and the temperature in the center of the compartment were monitored and are plotted on Figure 4. In comparison with Figure 1, it can be seen that, for extended periods of time, the 39% reduction in thickness of the Mg anode has a proportional effect on the hydrogen released, with virtually no uncombined Mg remaining for the thinner anode. The improved lateral conductivity, due to the exmet screen, actually speeds up the initial cell action and, correspondingly, both the rates of temperature increase and hydrogen release. This initial rate could be decreased, if desired, by either decreasing the amount of salt, or by bonding the exmet less firmly to the Mg.

Improvement of the Hot Sheet Through Utilization of Aluminum Alloy Anodes

Al, Zn, and Al Alloy Anode Polarization and Gas Evolution. For purposes of screening of a large number of samples, it was convenient to measure anodic polarization using a linear anodic potential sweep. The samples of 2 cm^2 area were fully immersed in a large volume of saturated NaCl solution thermostated at 25°C. The traces, of Figure 5, were obtained by starting at the respective rest potentials and sweeping toward positive potentials at a speed of 0.001 V/sec. Return sweeps (in the cathodic direction) were obtained after interrupting the anodic sweep manually at the approximate 200 mA/cm^2 level and then sweeping in the cathodic direction; the resulting traces appear in Figure 6. A comparison of Figures 5 and 6 reveals some hysteresis effect for pure Al and all of the alloys tested. This is not surprising considering the fact that Al is always

---

[17] J. L. Robinson, "Investigation of the Magnesium Anode," Proc. of 17th Annual Power Sources Conference, p. 142, May 1963.

VOLUME OF H_2 RELEASED (cc AT STP)

VOLUME OF H_2 RELEASED-
MODIFIED "HOT-SHEET"
○ UPPER TIME SCALE
□ LOWER TIME SCALE

TEMPERATURE IN CENTER OF FOOD PACKAGE
● EXPERIMENTAL "HOT-SHEET"
■ STANDARD "HOT-SHEET"

MINUTES
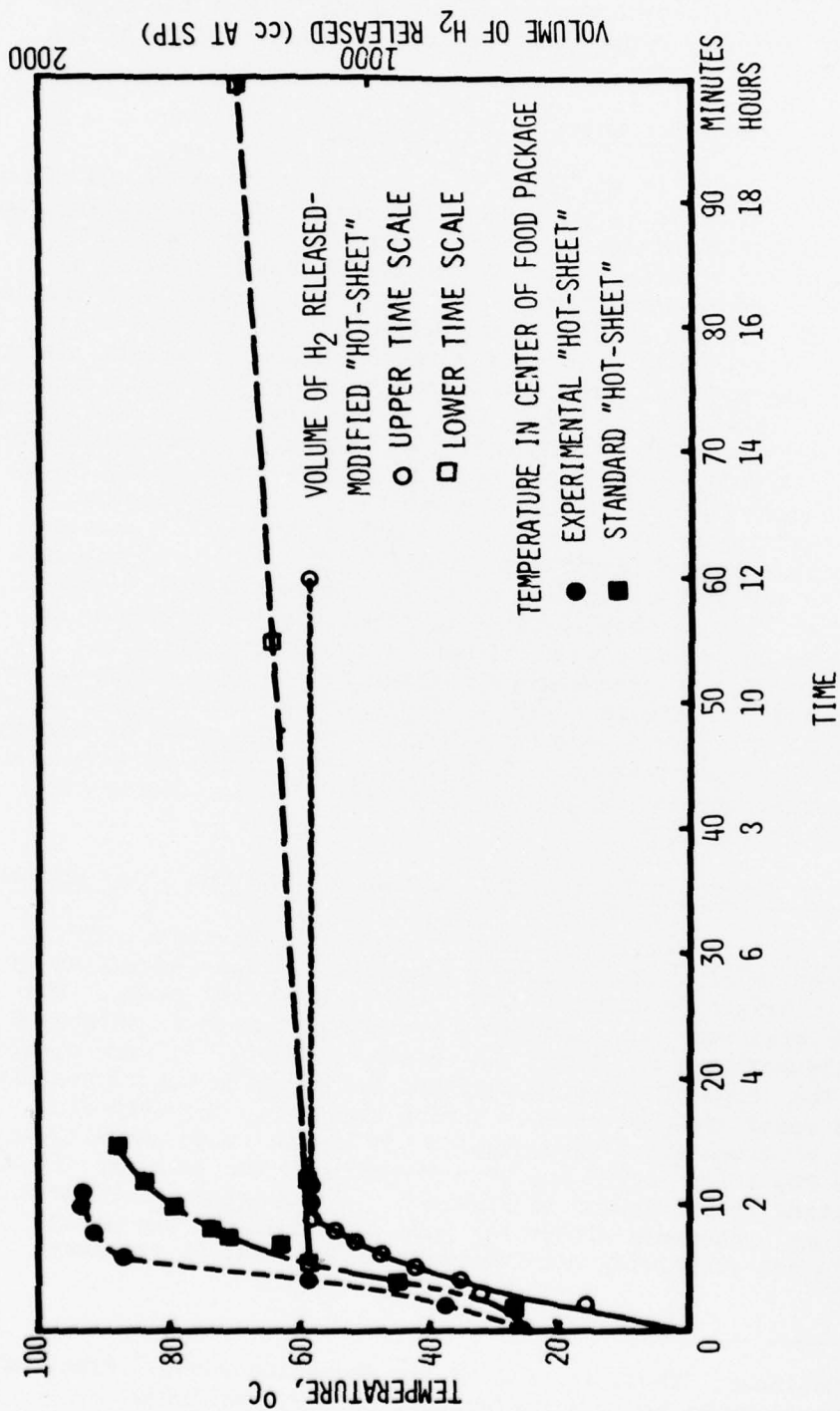HOURS

TIME

TEMPERATURE, °C

Figure 4. Comparative Performance of "Hot Sheets" With 0.028 cm (Standard) and 0.017 cm (Experimental) Thick Mg Anodes. Both "Hot Sheets" Were Wrapped Around a Standard Food Package.
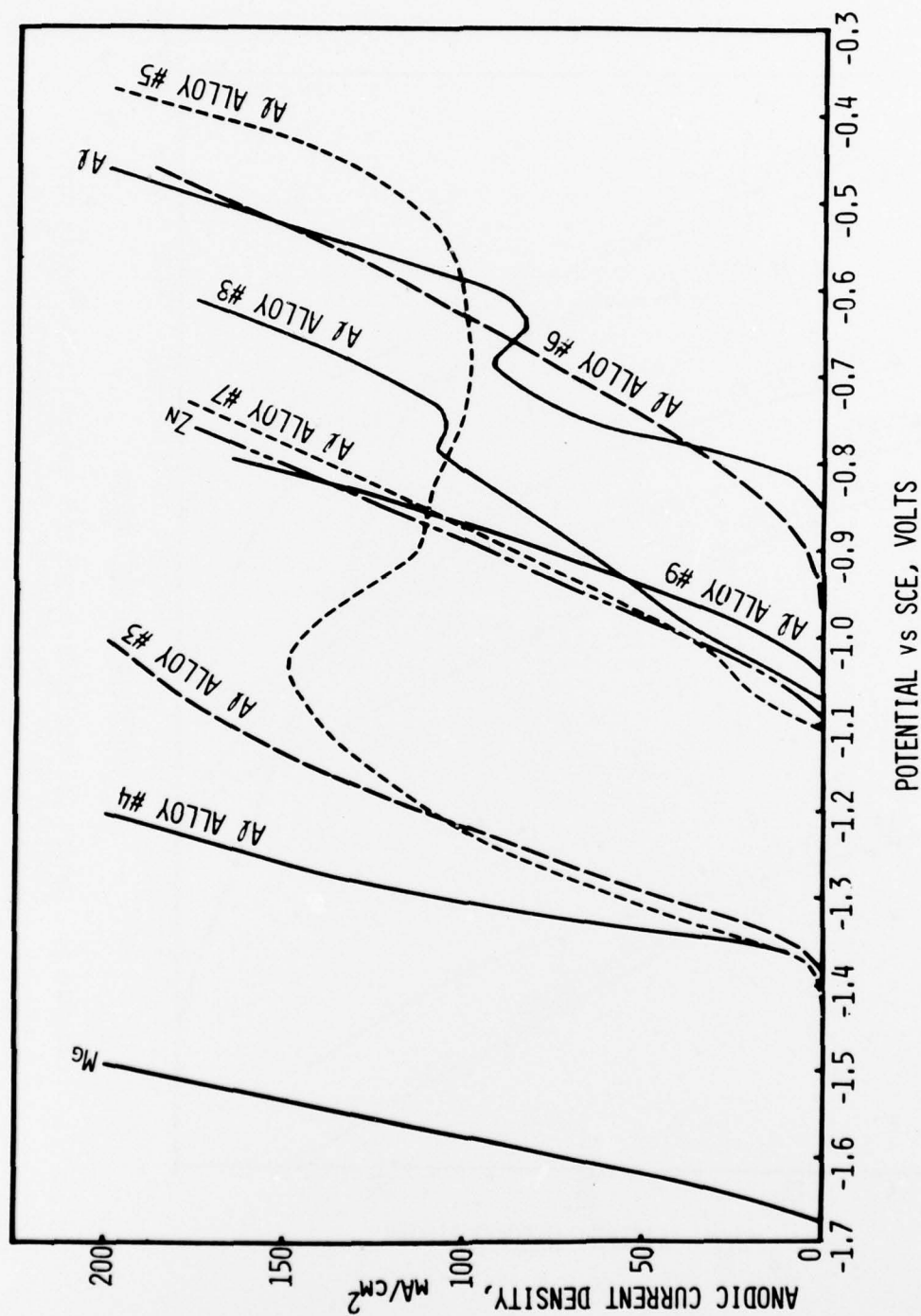
16

Figure 5. Anodic Polarization Curves for Several Pure Metals and
Aluminum Alloys in Saturated NaCl Solution at 25°C.
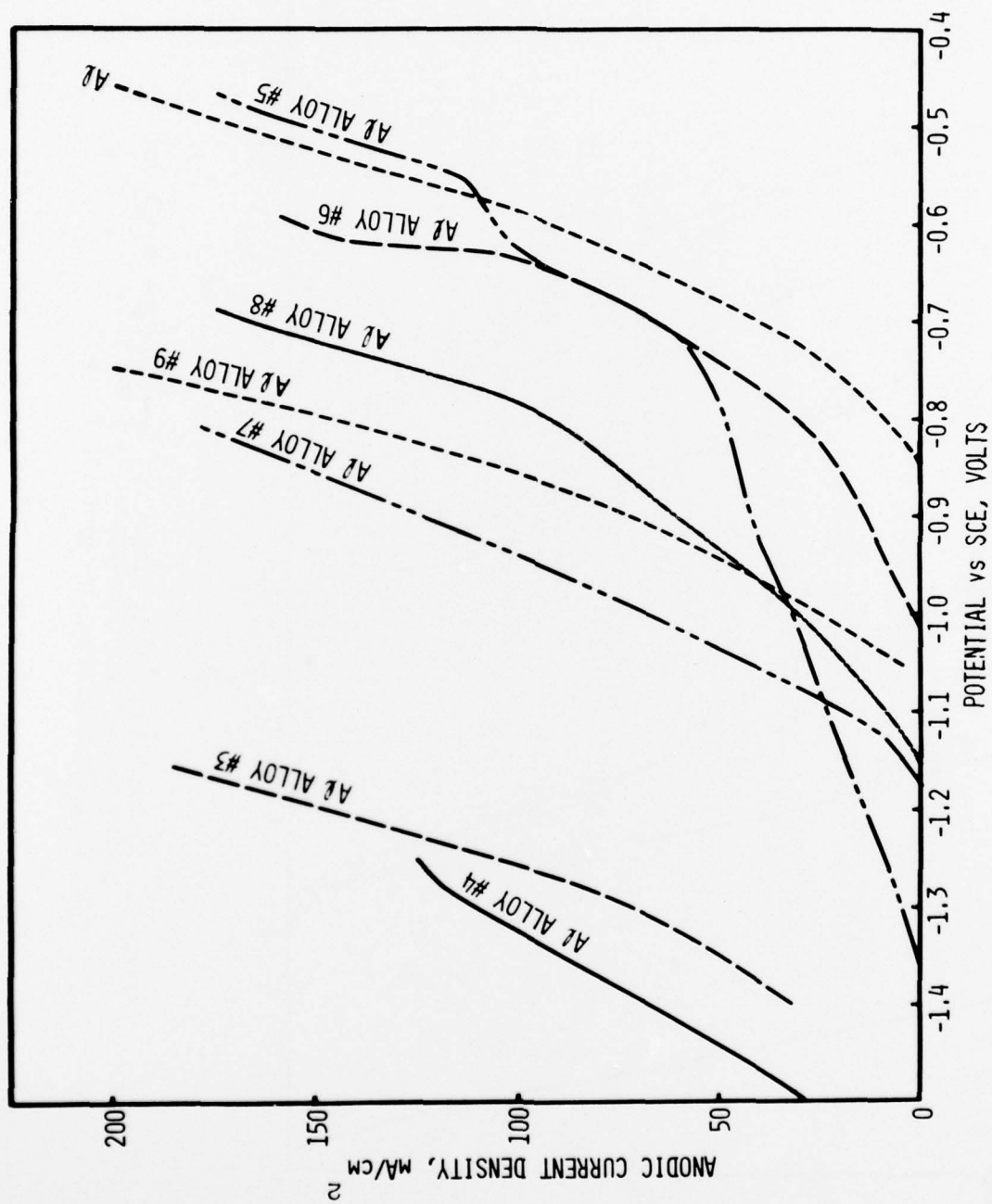Alloy Compositions are given in Table 3.

17

Figure 6. Anodic Polarization Curves for Several Pure Metals and Aluminum Alloys in Saturated NaCl Solution at 25°C. The Curves Were Obtained After Reversing the Linear Potential Sweeps of Figure 5.

18

covered with a film of γ-Al$_2$O$_3$ in near-neutral solutions,[18] that its electrochemical properties depend on the condition of that film, which in turn, depends on the previous history of the electrode. The behavior of any of the samples, as an electrochemical heater anode, may be expected to fall somewhere between the anodic and cathodic traces, since in practical use, the current densities are initially high and then undergo gradual decline.

For measurements of hydrogen evolved by the anode samples, it was convenient to impress the various constant current levels listed in Table 3. Measurements were made at one minute intervals for a total of eight minutes at each increasing current density. Table 3 presents the hydrogen evolution rate as a percentage of the total current at the anode, after converting the gassing rate to a current, I_{H_2}, by means of Equation (1). For current densities of 20 mA/cm^2 or higher, the gassing rates were found to stabilize after 2-3 minutes and the values given are average values for the last 4-8 minutes of observation. Since direct calibration revealed that a 2-3 minute lag is inherent in the flowmeter used for the measurements, no conclusions may be drawn about intrinsic transient behavior of the system in that period. For the alloys possessing low rates of gassing, the method was not sufficiently sensitive for observations to be made in the allotted time at the lowest current densities.

Referring to Figure 5 as a guide to the relative anodic behavior of the various anode materials, we see that the performance of the alloys falls into the approximate 1 volt span between Mg and pure Al, with the latter the more inactive material and with both operating much below their respective thermodynamic potentials as listed in Table 2. A trace for a Zn electrode is included for comparison, although the energy content of Zn is too low for practical consideration. A general pattern of behavior emerges for the alloys, if the high-current performance of alloy #5 is ignored. Those alloys (#3, 4, and 5) containing Zn produce the most negative (active) closed-circuit voltages. This is in agreement with observations[19,20] made during long-term corrosion studies on aluminum alloy/steel couples. It is believed[21] that Zn fosters the high anodic activity by producing cation vacancies which reduce the ionic resistivity of the γ-alumina film. This film normally covers the electrode during use. Additions of Mg and Ga enhance this effect by stabilizing the solid stability of the Sn in the alloy.[22] The H$_2$-evolution characteristics of alloys #3-5 tend to be somewhat better than that of pure Al, particularly at the high current densities, and like Al, are a 2-3 fold improvement over Mg in that regard. A second grouping of Al alloy polarization traces fall between the trace for pure Al and pure Zn (Figure 5). Alloys 6, 8, 7, and 9 contain increasing amounts of Zn and their closed circuit voltages, in

[18] D. S. Keir, M. J. Pryor, and P. R. Sperry, op. cit., p. 2.
[19] D. S. Keir, M. J. Pryor, and P. R. Sperry, op. cit., p. 2.
[20] J. T. Reding and J. J. Newport, Materials Protection, 15 (Dec.1966).
[21] J. T. Reding and J. J. Newport, op. cit.
[22] D. S. Keir, M. J. Pryor, and P. R. Sperry, J. Electrochem. Soc. 116, 319 (1969).

Table 3. Hydrogen Evolution at Magnesium, Aluminum, and Aluminum Alloy Anodes (25°C)

Composition No.	Anode Composition, Weight Percent							Percentage H_2 Evolution* I, mA/cm²					
	Mg	Al	Zn	Hg	Sn	Ga	In	5	10	20	50	100	200
1	100							43.6		45.3		38.7	36.9
2		100								13.4	16.9	19.8	15.9
3	0.57	99.25			0.13	0.05			8.6		16.8	16.3	6.9
4	0.82	99.98			0.15	0.05			17.7	14.1	14.5	13.8	
5	0.36	99.44			0.14	0.06			20.4	15.6	13.2	11.4	10.6
6		98.52	1.47	0.01						12.5	11.3		13.2
7	0.46	95.31	4.19				0.04				0.6	1.4	1.5
8		96.45	3.52				0.03				5.5	2.6	2.0
9		95.81	4.19						4.0	16.7	20.1	16.3	

* Percentage H_2 Evolution = $100 \, I_{H_2}/(I + I_{H_2})$

20

line with previous experience with Al-Zn alloys,[23] tend to become increasingly more negative, and approach the performance of a pure Zn anode. There is, however, no simple correlation between electrode polarization and hydrogen evolution for this series of alloys, if the results of Figure 5 and Table 3 are compared. Specifically, alloys #7 and #9 have the same Zn content and show very similar polarization behavior, but in spite of these facts, alloy #7 produces the lowest amount of hydrogen while hydrogen production for alloy #9 falls in the same range as for pure aluminum. The fact that alloy #8, like alloy #7, is also a low gas producer, suggests that Indium is more significant than Mg in imparting the non-gassing properties to those alloys. Before considering how alloying effects hydrogen evolution, let us consider the thermodynamics of the process. For gassing to occur at all, the electrode potential must be more negative than the thermodynamic value for a reversible H_2 electrode in the same medium. According to Table 2, that potential could be -0.650 V in the original neutral solution, and -0.597 V at steady state, with the solution completely equilibrated and saturated with hydrated γ-aluminum oxide. Based on those numbers, gassing would not be expected on pure Al or alloy #6 at the higher current densities. However, localized, very low pH values may be expected near the anode surface, particularly at high current densities, corresponding to the production and hydrolysis of $AlCl_3$. For example, based on the reported value of pKh = 4.9, the pH of a 1 M solution of $AlCl_3$ would be 2.45 and the corresponding reversible H_2 potential would be -0.38, sufficiently positive to account for H_2 evolution on Al and all of its alloys in a sodium chloride electrolyte solution. As for Mg, Table 3 reveals that the percentage of hydrogen evolved does not generally or systematically drop as the current is raised and the potential approaches that of the reversible H_2 electrode ("negative difference effect").[24] As for Mg, therefore, it may be hypothesized that H_2 release occurs on a very limited, momentarily film-free, fraction of the surface. In line with that concept, the role of Indium in a Zn-Al alloy could be to modify the physical structure of the film (e.g., adherency, coherency, porosity) so as to minimize exposure of bare surface to the electrolyte.

We shall now turn to the problem of choosing the "best" anode material for an electrochemical heater. From the point of view of lower H_2 production, Table 3 reveals that alloy #7 appears to be the best choice, with #8 a close second choice. Assuming that the solid product of reaction is γ-alumina for both Al and all of the Al-rich alloys, the total heat produced per equivalent of Al consumed, in short-circuited cells utilizing any of those anodes and a MnO_2 cathode, should be greater for the alloys producing the least H_2 (since reaction 3 of Table 1 is more energetic than reaction 4). In spite of that analysis, the anode polarization (see Figures 5 and 6) must be taken into account in the final choice of the alloy in three important ways:

(1) The distribution of heat through the cell depends on the relative extents of anode and cathode polarization and of electrolyte resistance. Since the anode is normally placed against the food packet, it is actually beneficial to have the highest polarization (and temperature) at that electrode.

---

[23] J. T. Reding and J. J. Newport, op. cit., p. 19.
[24] J. L. Robinson and P. F. King, op. cit., p. 14.

(2) The rate of heat release is proportional to the current density. That rate (or current) depends on the points of intersection of the anode and cathode polarization curves, as already explained for the Mg/MnO$_2$ cell.

(3) The anode polarization curve helps establish the working potential of the cathode at short circuit. The more positive the anode potentials (and the cathode working potential), the more likely will be the avoidance of H$_2$ evolution at the cathode. The latter has already been shown to be largely responsible for longer-term gas evolution.

Consideration (2) above suggests that the alloy should have a polarization curve as close as possible to that of Mg, in order to maintain a high internal current (e.g., by the use of a Sn-Al alloy such as #3 and #4 of Figure 5 which unfortunately is also high-gassing) whereas considerations (1) and (3) suggest that the polarization curve should be as far as possible to the right of Mg (e.g., the low-gassing Zn-alloy #7 of Figure 5). In order to resolve these conflicting requirements, it was necessary to attempt improvements in the polarization characteristics of the cathode, as described in the section below.

Screening of New Cathode Formulations. From Table 2 it can be seen that the reversible potential of the MnO$_2$ electrode is +0.364 V in the originally neutral solution used here as the electrolyte. Variations in pH during cell discharge can be expected to affect the reversible potential by only a few tenths of a volt. In spite of this, the present "hot-sheet" cathode begins to deliver appreciable cathodic currents at potentials over a volt more cathodic than the reversible potential. Such irreversible performance is subject to improvement through structural modifications which decrease internal impedances and improve mass transport in the electrode. Toward that end, a number of different electrode formulations were made for evaluation. These formulations included variation in (1) the amount of carbon and graphite added for contact between MnO$_2$ particles, (2) nature of the organic binder (e.g., PTFE, lucite polysulfone), (3) addition of agents to increase wetting and porosity (e.g., Fullers Earth) nature of the current collector (e.g., screens and expanded metal made of steel and nickel), and (4) the addition of graphite fibers to improve current collection.

For evaluation of samples, the potential-step method, as used to obtain the data of Figure 3, provides the most in-depth information, but requires multiple samples and is tedious. Therefore, for the present purpose of fast screening, the linear potential sweep method requiring only one sample for a determination, was used instead (sweep speed of 0.001 V/sec.). Samples of 1 cm x 1 cm dimensions were discharged against a Mg counterelectrode using a section of the standard "hot sheet" electrolyte pad containing NaCl. Some of the more promising results appear in Figure 7. Formulations #2, #3, and #4 all offer the promise of improved performance at more positive potentials as compared with the standard "hot-sheet" cathode. All three improvements utilize lucite or polysulfone in place of PTFE as the binder and utilize graphite fiber additions. Formulations #2 and #3 were made with a steel screen current collector, while #4 was made with a "foametal" current collector. While cathode performance increases on progressing from
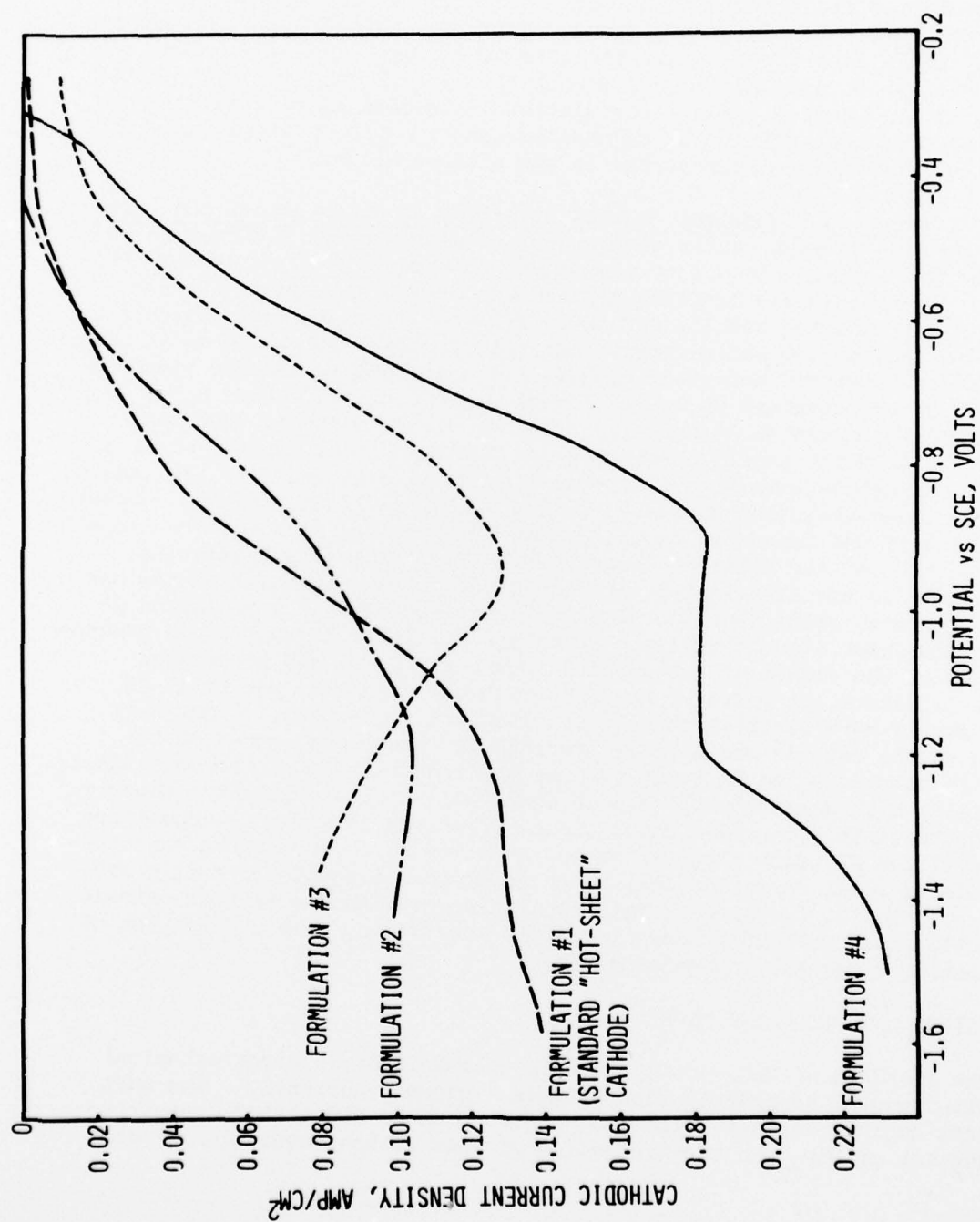
FORMULATION #3

FORMULATION #2

FORMULATION #1
(STANDARD "HOT-SHEET"
CATHODE)

FORMULATION #4

POTENTIAL vs SCE, VOLTS

CATHODIC CURRENT DENSITY, AMP/CM²

-0.2 -0.4 -0.6 -0.8 -1.0 -1.2 -1.4 -1.6

0 0.02 0.04 0.06 0.08 0.10 0.12 0.14 0.16 0.18 0.20 0.22

Figure 7. Cathodic Voltage Scans of Various MnO₂ Cathodes.
The Electrolyte was NaCl Solution in a Webril Pad.

23

formulation #1 to #4, so does the MnO_2 loading (0.035, 0.07, 0.17, and 0.2 g/cm^2 for electrodes 1, 2, 3, and 4, respectively). Hence, the improvement represents successful utilization of more MnO_2, rather than a fundamental improvement in the kinetics of MnO_2 reduction. From Figure 7, formulation #4 would appear to be the obvious choice for further development. Its vulnerability, however, is the fact that Ni is a rather good catalyst in the H_2 evolution reaction. The descending portion of the scan from -1.2 V to more cathodic potentials corresponds largely to extensive gas production, which is significant even at more positive potentials. An electrochemical heater using that formulation was, nevertheless, evaluated and the results reported in the section below. Formulation #3 appears clearly superior to the standard cathode without an aggravated gas evolution problem, and its further evaluation is also reported in the section below.

Prototype Electrochemical Heaters Utilizing Al Alloy Anodes and Improved MnO_2 Cathodes. Complete cells were assembled using Webril electrolyte pads saturated with NaCl, 1 cm x 1 cm electrodes, and small MnO_2 reference electrodes. Electrochemical measurements and gas evolution were monitored simultaneously and the results appear in Figures 8-10. Figure 8 reveals that, as expected, the short circuit current of a cell utilizing an Al alloy anode and the standard hot-sheet cathode, is considerably reduced compared with that of the standard Mg cell. Figure 9 shows that the same alloy used with cathode formulation #3 actually provides higher currents than the standard cell, which should compensate for the lower heat content of this couple. Comparison with Figure 2 reveals a dramatic decrease in the gassing rate ("hydrogen-evolution current") during the first 15 minutes and complete elimination of the long-term gassing which, as we have seen, occurs largely at the cathode of the standard "hot-sheet." The latter improvement is attributable to the anticipated more positive cathode potential of the new cell. Figure 10 shows that the Al alloy used with cathode formulation #4 can provide short circuit currents which are initially several times greater than that of the standard "hot-sheet." However, the H_2 gas production problem is severe, in spite of the fact that the electrode potential is significantly more positive than in the standard "hot-sheet." Long-term gassing at the cathode was already predictable (see above) based on the catalytic nature of the Ni exmet used in the construction of the new cathode. The initial high gassing rates appear anomalous at first thought. However, Ni is quite visibly corroded under these circumstances. The re-deposition of solubilized Ni salts directly on the Al alloy surface could be expected to produce a local corrosion cell which could then account for a high rate of H_2 evolution at the anode. This result suggests that a similar cathode formulation made without Ni may ultimately provide the best combination of high heating rates and low gassing rates.

CONCLUSIONS AND RECOMMENDATIONS

The standard $Mg-MnO_2$ hot sheet is a short-circuited electrochemical cell with several separately identifiable "internal currents." The most important current is that which flows between anode and cathode resulting in reduction of MnO_2 and the production of heat without evolution of gas.

24

Figure 8. Operating Characteristics of an Electrochemical Heater Made With an Al Alloy #7 (4.19% Zn, 0.04% In, 0.46% Mg) Anode and a MnO_2 Formulation #1 (Standard) Cathode.
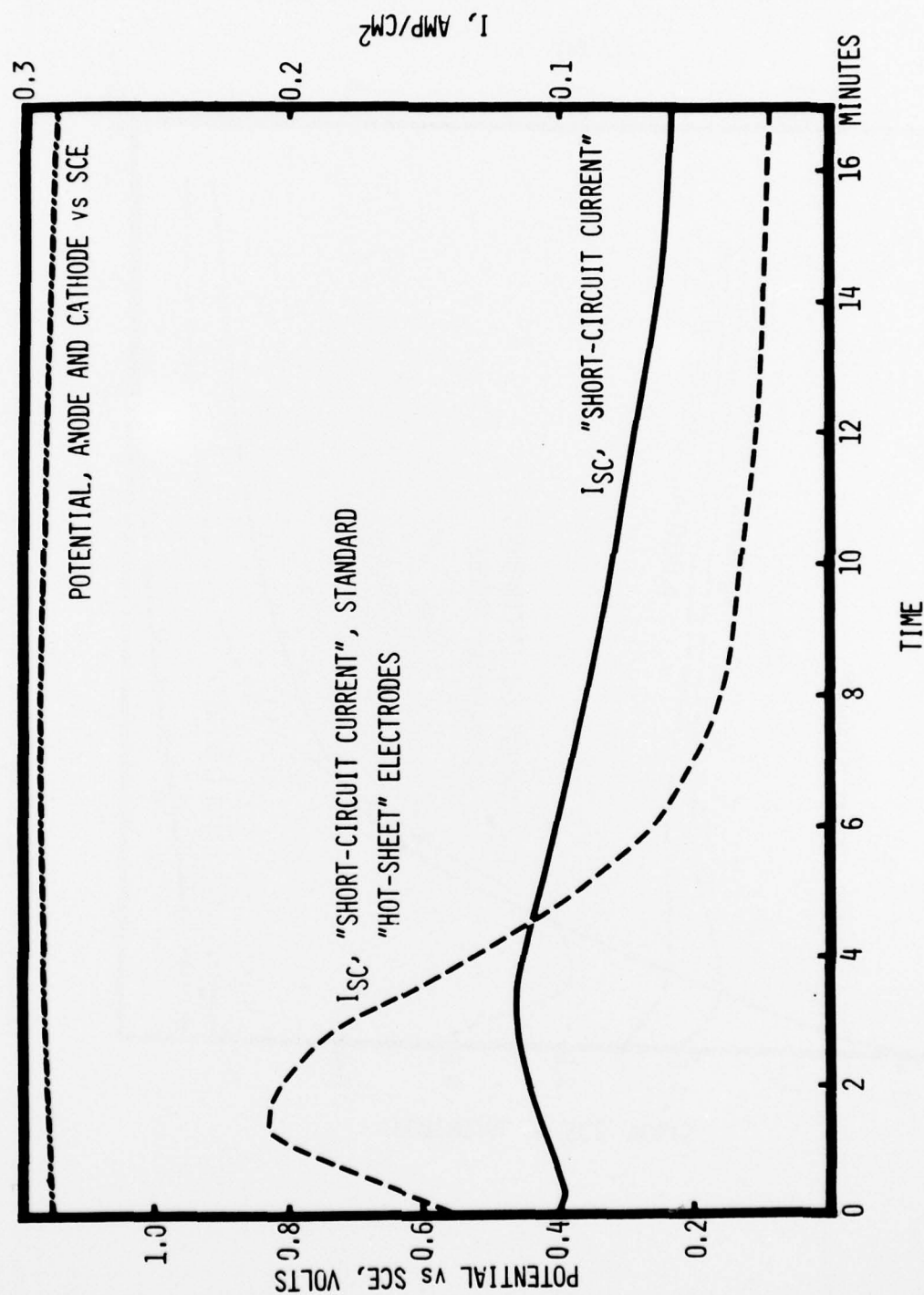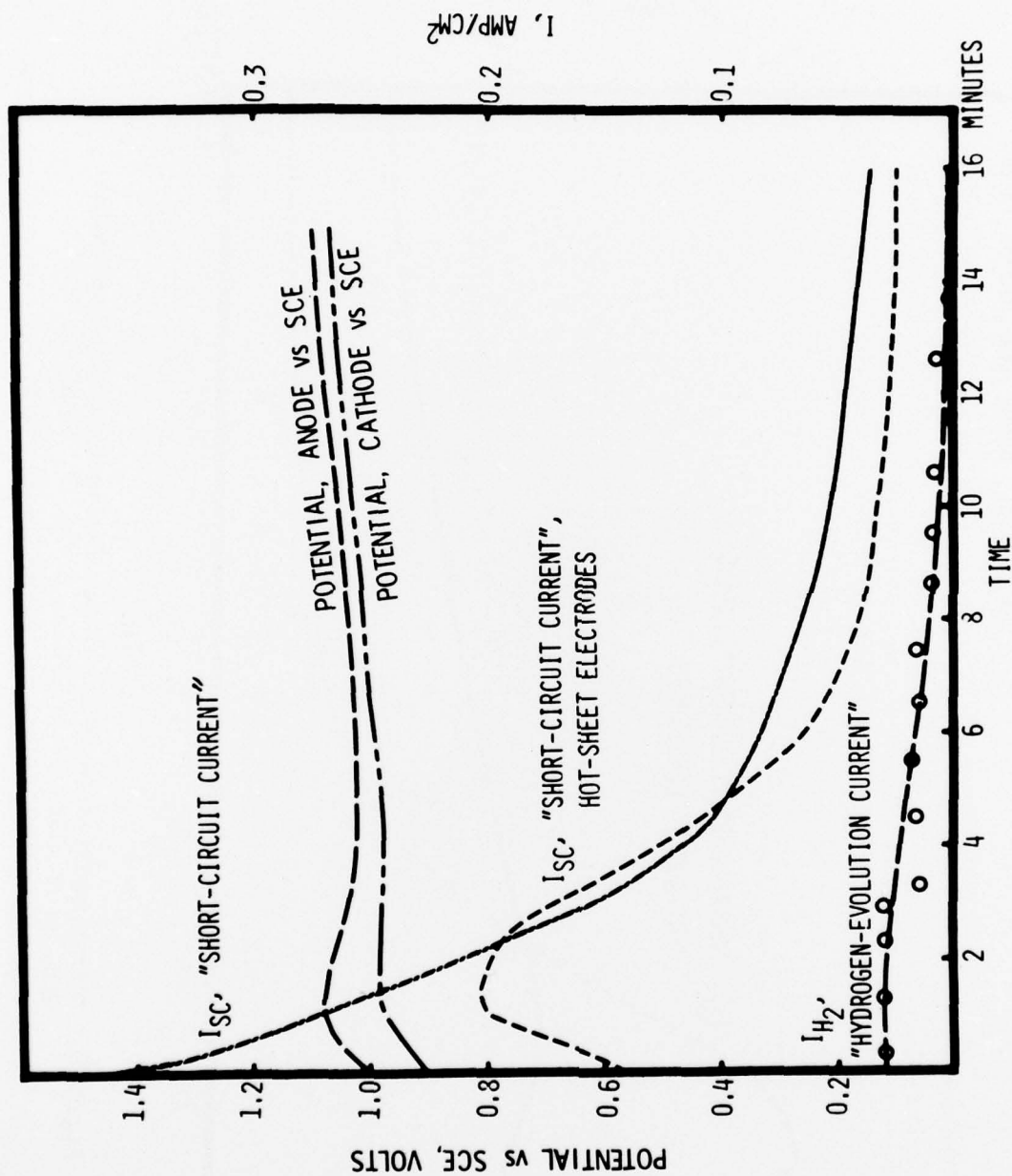
25

Figure 9. Operating Characteristics of an Electrochemical Heater Made With an Al Alloy #7 (4.19% Zn, 0.04% In, 0.46% Mg) Anode and a MnO₂ Formulation #3 Cathode.
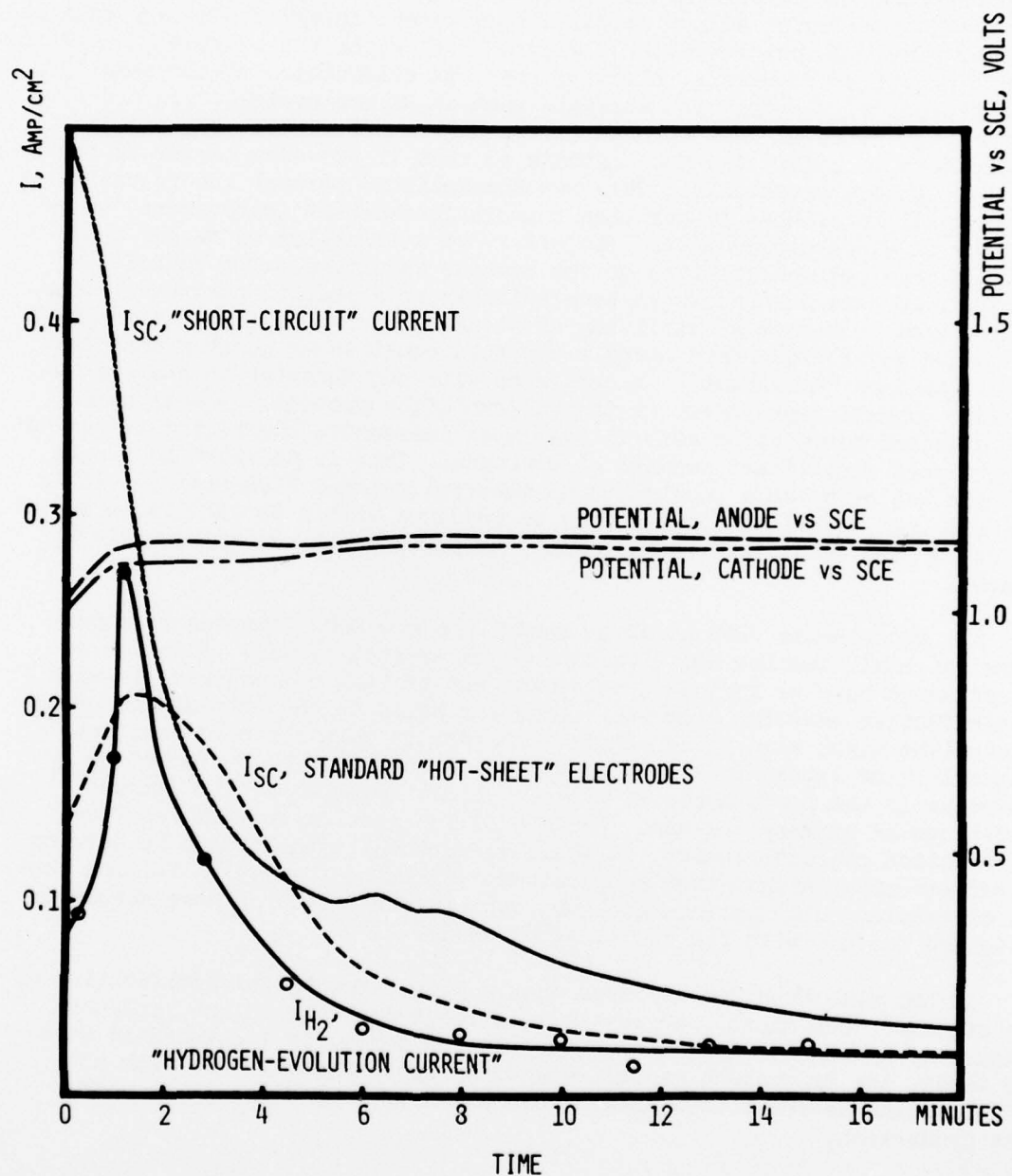
Figure 10. Operating Characteristics of an Electrochemical Heater Made With an Al Alloy #7 (4.19% Zn, 0.04% In, 0.46% Mg) Anode and a MnO2 Formulation #4 Cathode.

27

A second current flowing between the two electrodes produces a smaller quantity of heat per coulomb of Mg consumed and is responsible for long-term evolution of hydrogen gas at the cathode. A third "corrosion" current is localized to the anode and is responsible for most of the hydrogen released by the "hot sheet" during the first several minutes of use. The corrosion rates of certain Al alloys containing In and Zn are very much less than that of Mg, which allows dramatic improvement in the short-term gassing problem. The high polarization of such alloys causes the cathode to operate at more positive potentials, allowing complete elimination of the long-term gassing problem if catalytic materials such as Ni are avoided. In order to realize high rates of heat release (i.e., high short circuit currents), it is necessary to modify the MnO_2 cathode so that it provides larger currents at less cathodic potentials. This was accomplished through incorporation of larger loadings of MnO_2 rather than through fundamental improvements in the kinetics of electro-reduction. The effective utilization of larger MnO_2 loadings required modification of the cathode structure. Two cathode formulations have been shown to have suitable polarization characteristics. Miniaturized "hot-sheets" utilizing an Al alloy and these formulations have been shown to provide short circuit currents equal to or greater than that of the standard "hot-sheet." A cell made with one formulation shows a dramatic overall improvement in the gas-evolution problem. A cell made with a second formulation affords even more impressive short-circuit current, but produces significant amounts of hydrogen. This is believed to result from the use of Ni as a constructural material (nickel "foametal"). It is possible that a similar foametal may be produced with a Ni substitute so as to retain good electrical (and thermal) properties without appreciable H_2 release.

All experiments with Al alloy anodes and new MnO_2 cathodes were performed on small samples and with external electrical leads. A follow-on effort would have to include development and testing of larger cells with cost-effective shorting elements. Some variation in the composition of the electrolyte might also be beneficial in order to obtain a more constant, longer lasting internal current flow. Tests must also be performed to determine if the performance of the new alloys is sensitive to extreme conditions of storage and use. Because of its particularly impressive polarization characteristics, it would be worthwhile to attempt to develop a cost-effective nickel-free MnO_2 cathode utilizing foametal. Failing that, the alternative high performance MnO_2 structure reported on here should be optimized for use with the new Al alloy anode.

It has also been demonstrated that a purely mechanical modification of the standard "hot sheet" can result in a large decrease in the long-term release of hydrogen. If a current-collecting screen is incorporated into the anode, the Mg content can be reduced by approximately 40%, with a corresponding decrease in hydrogen volume and with no decrease in useful heat production.

ACKNOWLEDGMENT

HISA-FM-1749-77